Journal of Materials Physics and Chemistry, 2018, Vol. 6, No. 1, 9-16
Available online at http://pubs.sciepub.com/jmpc/6/1/2

DOI:10.12691/jmpc-6-1-2

Photovoltaic Properties of Aluminum Doped Zinc Oxide Electrodes Based on Variation of Aluminum Impurities in the Semiconductor

M. D. Tyona[1,*], R. U. Osuji[2], C. D. Lokhande[3], F. I. Ezema[2]

[1]Department of Physics, Benue State University, P.M.B. 102119, Makurdi, Nigeria
[2]Department of Physics and Astronomy, University of Nigeria, P.O. Box 2201, Nsukka, Nigeria
[3]Department of Physics, D Y Patil University, Kolhapur, (M S) India
*Corresponding author: Dtyona@gmail.com

Abstract Photoelectrochemical (PEC) solar cell studies of Al doped zinc oxide (AZO) thin film electrodes has been carried out by photocurrent-voltage (I-V) characteristic. The concentration of Al in ZnO was varied between 1-5 at.% in order to study the effect of the variation on the photovoltaic performance of the electrodes. The current-voltage (I-V) characteristics measured in the dark and under 80 W simulated illumination revealed enhanced PV performance for the AZO electrodes in contrast to the undoped electrode. The best response was achieved for AZO electrode with 2 at.% Al concentration thus, recording higher conversion efficiency and fill factor. This is a clear indication that AZO electrodes are superior to undoped ZnO in PV applications. The remarkable enhanced properties of Al doping on ZnO were carefully studied by means of thickness measurement, X-ray diffraction (XRD), scanning electron microscope (SEM) and UV-Vis spectroscopy, and the results were in good agreement, and confirmed that AZO thin film electrodes are better for PV applications than undoped ZnO semiconductor in sodium sulphate (Na_2SO_4) electrolyte.

Keywords: *AZO electrode, Photoelectrochemical, Al concentration, chemical bath deposition, X-ray diffraction, film thickness*

Cite This Article: M. D. Tyona, R. U. Osuji, C. D. Lokhande, and F. I. Ezema, "Photovoltaic Properties of Aluminum Doped Zinc Oxide Electrodes Based on Variation of Aluminum Impurities in the Semiconductor." *Journal of Materials Physics and Chemistry*, vol. 6, no. 1 (2018): 9-16. doi: 10.12691/jmpc-6-1-2.

1. Introduction

Scientific development in materials technology over the last few decades realizes the usage of wide-band gap semiconductors for various optoelectronic device applications including photovoltaic (PV) solar cells [1]. ZnO semiconductor is an attractive material in the research community for photoelectrochemical (PEC) solar cells due to its wide, direct band gap (E_g -3.37 eV at 300 K), and large exciton binding energy (60 MeV), large non-linear optical coefficients, high thermal conductivity and excellent electrochemical stability [1,2]. However, the large photonic energy requirement of ZnO semiconductor (about 3.2-3.37 eV) only limits its light absorption with in a small fraction of the solar spectrum [3]. Thin film properties such as crystal structures, surface structures, band gap and optical absorption and electrical/optical conductivity of ZnO has been improved by introducing dopants in to ZnO lattice [4]. The transition metals (Al, Cu, Ni, Ag, Co) doped ZnO show better properties which are suitable for photovoltaic (PV) application, as these metals have ionic radius nearly similar to ZnO [5,6]. Al^{3+} has been the most used dopant element due to its small ionic radius and low material cost. Al doped ZnO (AZO) nanostructures are used in transparent conductive plates due to its high optical conductivity and transparency in the visible region [7,8]. The substitution of Zn^{2+} ions with Al^{3+} in ZnO lattice improves the electrical conductivity through the increase of charge carriers where it is reported that the electron concentration increases from 1016 to 1021 cm^{-3} [9,10].

The challenge in converting sunlight into electricity via photovoltaic solar cells is to lower the cost per watt of delivered solar electricity to the barest minimum [11,12]. PEC solar cell is a recent PV technology that is aimed at delivering solar electricity at a reasonably low cost by utilizing low cost materials in thin films and adopting inexpensive materials synthesis and cell fabrication techniques [13]. Nanocrystalline semiconductor thin film electrodes are the key components of PEC solar cells due to their large effective surface area available for absorption of electrolyte, which facilitates rapid electron transport in the electrode and thus, enhances power conversion efficiency and sustainable power [14].

PEC conversion of sunlight to electrical power was first achieved with a TiO_2 semiconductor photoelectrode in a pioneer work reported by Grätzel [15]. ZnO semiconductor was discovered later as an effective counterpart of the former [16,17]. Nevertheless, TiO_2 nanoparticle films with transparent conducting oxide (TCO) layers are used as

photoelectrode in PEC solar cells because of their adequate surface area and chemical affinity for electrolyte absorption as well as their suitable energy band potential for charge transfer between the photoelectrode and electrolyte. However, the numerous grain boundaries between the TiO_2 nanoparticles restrict fast electron transport, which is detrimental to carrying out a highly efficient energy conversion process [18]. ZnO nanostructured photoelectrodes have been confirmed to improve the electron transfer by virtue of eliminating the grain boundaries [18]. Furthermore, the charge carrier concentration and mobility and hence conductivity of ZnO can be improved in order to enhance it's PEC performance [19]. Doping ZnO with Al, has been one of the effective methods to enhance the conductivity of ZnO. There has been quite a bit of literature on Al-doping of ZnO which successfully enhanced it's conductivity [18,19,20,21]. However, there has not been enough focus on the application of such AZO materials in PEC solar cells in the available literature. Therefore, in this paper, PEC properties of AZO electrodes synthesized by a novel chemical bath deposition (CBD) technique, with varying concentration of Al is reported.

2. Experimental Details

AZO thin films were synthesized in a chemical bath according to our previous work [14]. Firstly, an aqueous solution of 0.1 M $Zn(NO_3)_2.6H_2O$ (sd fine chemicals) was prepared. To achieve aluminum doping, aluminum nitrate ($Al(NO_3)_3.9H_2O$; Lobo Chemie-India) was added to the solution. The doping concentration, i.e., Al/Zn atomic ratio was varied from 1 to 5 at.% in the solution.. Concentrated ammonia solution (NH_3; Thomas Baker, 28% in H_2O) was used to adjusted the pH of the solution under constant stirring at room temperature. A white precipitate of $Al\text{-}Zn(OH)_2$ was initially observed, which was soluble in excess NH_3 solution. The alkaline bath was maintained at a pH~11.5. Ultrasonically cleaned microscope glass slide and stainless-steel substrates were immersed vertically in the solution using Bakelite holders (Figure 1) and the bath temperature was maintained at 353 K. The substrates coated with AZO thin film were removed after 5 h, washed with double distilled water dried in air and preserved in the vacuum desiccator. Further, as-deposited films were air annealed at 673 K for 2 h.

PEC properties of the films were studied in a three-electrode, single compartment cell (n-AZO (on stainless steel substrate) as a photoelectrodes, Platinum wire as counter electrode and saturated calomel electrode (SCE) as the reference electrode in 0.1 M Na_2SO_4 solution as the electrolyte) in an electrochemical workstation as illustrated in Figure 7 (a). An 80 W xenon arc lamp was used as a simulated white light to illuminate a semiconductor photoelectrode area of 1 cm^2. Film thickness of the synthesized AZO thin films was analysed with a surface profilometer (AUB 105 Technology, Model XP-1). Optical properties of the films were recorded with a Shimadzu, UV-1800 spectrophotometer. Structural properties were studied using Philips PW 1830 X-ray diffractometer with CuKα radiation (λ = 1.5406 Å) in the range of 20 – 80° in 2θ. Surface morphology was studied with scanning electron microscope (SEM) using JEOL JSM-6360.

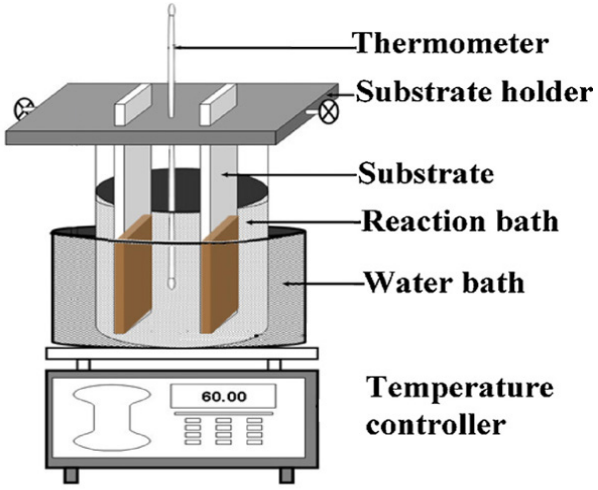

Figure 1. Schematic diagram of the experimental setup for deposition of AZO thin films by chemical bath deposition technique

3. Results and discussion

3.1. Film Thickness Characterization

Film thickness is one of the most significant parameters that affect the properties of thin films. Determination of film thickness is of much importance for quantitative evaluation of certain film parameters and applications. For PEC solar cell application, the typical film thickness for optimal light energy to electrical energy conversion efficiency is in the range of 8 -12 μm [22]. Figure 2 shows the variation of AZO film thickness with deposition time at constant bath temperature (353 K) measured in this work using surface profilometer (AUB 105 Technology, Model XP-1). The results indicate that the development of film thickness is time dependent. As the temperature of the heated bath gradually rises to 353 K, precipitation begins in the solution and metal ions are slowly released to form thin solid film of AZO on the substrate. It is also clear from Fig. 2 that the growth rate of the films strongly depends on the concentration of dopant, Al in the solution [23]. This could be assigned to the fact that introduction of the dopant increases the number of free metal ions in the solution which facilitate rapid growth of the films [22,23].

A careful study of the growth mechanism of AZO by CBD method reveals that, when the alkaline zinc nitrate bath was heated up to a temperature of 353 K for a period of about 1 h, precipitation starts and deposition of AZO begins by heterogeneous reaction at substrate surface and the film thickness increased with time. The deposition time was varied between 2 and 5 h (Figure 2). It was observed that at the initial stage of the deposition process, the film growth rate was rapid, showing an increase rate of about 0.21-0.28 nm/min however, after 4 h, the growth rate became slower until final thickness was obtained at 5 h. This could be ascribed to decrease in number of free metal and chalcogenide ions in the solution [22,24]. Measured values of the film thickness and surface roughness are presented in Table 1.

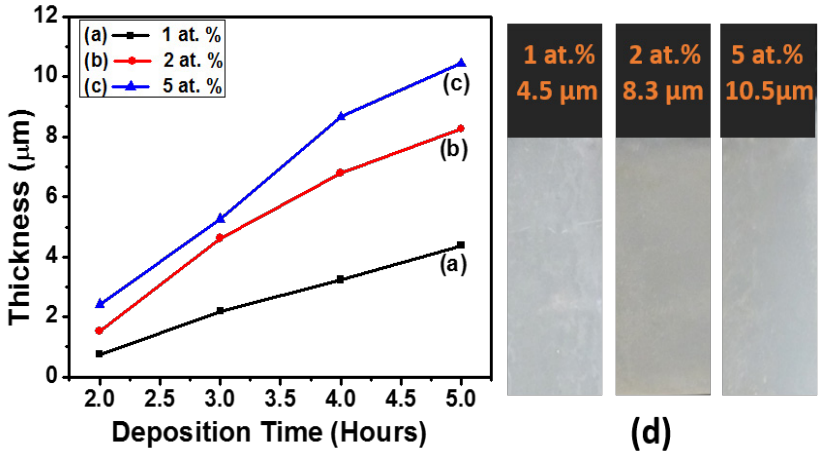

Figure 2. AZO film thickness variation with deposition period for different Al concentrations (a) 1 at. % (b) 2 at. % and (c) 5 at. % (d) photographs of the annealed synthesized AZO thin film with different Al concentrations

Table 1. Measured film thickness and surface roughness of AZO with different Al concentrations

AZO Electrodes with % Al	Thickness (μm)	Surface Roughness (nm)
0	5.50	162
1	7.78	148
2	8.87	152
5	10.15	154

3.2. Structural Characterization

Figure 3 illustrates the XRD patterns of AZO thin films annealed at 673 K. All the films were seen to be polycrystalline with hexagonal wurtzite structure, showing diffraction peaks, which were well indexed to ZnO (JCPDS File No. 00-036-1451), with lattice constants a=3.24982 Å and c=5.20661Å correspondingly. From the XRD patterns, sharp characteristic peaks were indexed to the crystal faces (100), (002), and (101) at 32.1°, 34.7°, and 36.6°, with highly oriented c-axis of high intensities for the film samples with Zn:Al of 0 and 2 at. %, which is the densest plane in wurtzite ZnO [25]. However, for AZO films with Zn:Al of 1 and 5 at. %, the diffraction peaks were highly diminished [12,14].

The decrease in intensity of the *c*-axis peak on incorporation of Al into ZnO (ie Al/Zn = 1 at.%) as observed (Figure 3b) could be attributed to the fact that the introduction of Al impurities in ZnO might have induced some crystallographic defects which results to the contraction of the *c*-axis and hence reduce the crystallinity of the film. However, increasing the concentration of Al to 2 at.% enhances charge carrier concentration and mobility in the conduction band of the semiconductor [26,27], thereby reducing the amount of crystallographic defects in the film. This result suggests that the crystalline quality of the film in the ZnO (002) plane for this concentration of Al would improve significantly as demonstrated in Figure 3 (c) [20,21]. As the Al concentration was further increased to 5 at.%, the crystallinity of the film decreased sharply. This is an indication that there is more compressive strain in the films at higher doping level [26]. Additionally, according to Barna and Adamik structure zone model for polycrystalline metallic films level [26], as the impurity content is increased, there is more segregation of impurities at the grain boundaries of the film which result in lowering of grain sizes [20,26] which is similar to the case observed here. This implies that 2 at.% Al concentration could be the optimum concentration of Al in ZnO for the best crystalline quality film of AZO thin films. This observation is a slight deviation from earlier reports available in some literature even though they used different synthetic techniques and concentration of Al [20,21,26].

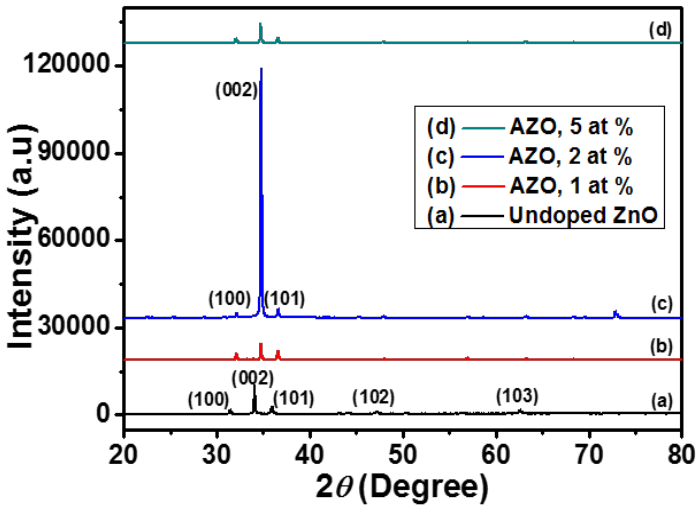

Figure 3. XRD patterns of AZO with different Al concentration. (a) 0 at.%. (b) 1 at.%. (c) 2 at.%. (d) 5 at. %

The XRD patterns further indicates a diffraction peak shift of 0.6° in 2θ towards the higher angle for all AZO films as depicted in Figure 3 (b)-(d). This may be assigned to the decrease in crystallite size associated with the diffusion and replacement of Zn with Al, with difference in ionic radii of Zn^{2+} and Al^{3+} (which is higher for Zn^{2+} as compared to Al^{3+}) such that the length of the *c*-axis is expected to be shorter when Al atoms are substituted into Zn sites in the crystal lattice [26,27].

Mean crystallite size of the AZO thin films were estimated along the (002) crystal plane on the basis of full width at half maxima (FWHM) using Scherrer's formula [14,28]:

$$D = \frac{0.9\lambda}{\beta \mathrm{Cos}\theta} \quad (1)$$

where λ, β, and θ are the X-ray wavelength (λ =1.54056 Å), full width at half maximum (FWHM) and diffraction peak angle, respectively. The estimated crystallite sizes showed that the mean crystallite size of ZnO film increased from 28 to 29 nm as presented in Table 2.

Table 2. Estimated crystallite sizes of AZO thin films along (002) crystal plane

% Doping of Al	Mean crystallite size (nm)
0	28
1	16
2	29
5	18

3.3. Surface Morphological Studies

The SEM images of AZO thin films annealed at 673 K are depicted in Figure 4. It is clearly seen here that the morphology of the AZO is significantly affected by the concentration of Al in the semiconductor. The crystallite sizes and porosity of the films decreases upon introduction of the dopant, Al as was suggested by XRD study. This behaviour could be assigned to the difference between the ionic radius of Zn and the doping elements, Al [4,14,18]. The undoped ZnO (as reference, Figure 4a) shows fibrous nano-dendrites, well indexed to wurzite ZnO with mean rod size of ~28 nm. On incorporation of Al impurities into the semiconductor (Al/Zn = 1 at.%), the nano-dendritic structures became more refined however, a critical lowering in the mean diameter of the dendritic rods occur (Figure 4b), which is in good agreement with XRD result.

By increasing the Al concentration to 2 at.%, the nano-dendrite morphology became denser, with well-defined and nearly uniform rod sizes (rod diameter of ~29 nm) as illustrated in Figure 4(c). This is a demonstration of an improved crystalline quality as earlier suggested by XRD result. This kind of morphology is very suitable for PEC solar cell application. Further increase in the concentration of Al to 5 at.% as shown in Figure 4 (d), the SEM micrographs of AZO in contrast to the results of 1 and 2 at.% were transformed to dense and randomly oriented nanorods of average diameter ~17 nm. This observation agrees with that observed by Lee et. al and Becerril et al using pulsed laser deposition and co-sputtering synthesis of AZO thin films respectively [4,18].

3.3. Optical Characterizations

Figure 5, illustrates the optical absorption spectra of Al-doped ZnO thin films for various Al concentrations. The absorption spectra revealed that all AZO films exhibited low absorbance in the visible region (from 400 nm) especially for the sample with Al:Zn = 1 at.%. However, the absorption edge for AZO films with 2 and 5 at.% Al concentrations were red-shifted (to 430 and 450 nm, respectively). This could be attributed to the enhancement in optical properties induced by Al doping [29,30,31].

Figure 4. SEM micrographs of AZO thin films for different Al concentrations. (a) 0 at.% (b) 1 at.%, (c) 2 at.% (d) 5 at.%

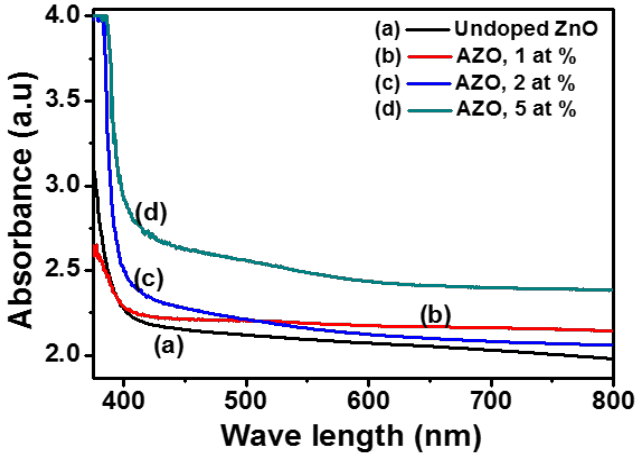

Figure 5. Absorption spectra of AZO thin film for different Al concentrations. (a) 0 at.%. (b) 1 at.%. (c) 2 at.%. (d) 5 at.%

The optical band gap energy (E_g) was estimated from Tauc plot (Figure 6) using Tauc's relationship between the absorption coefficient, α, and the photon energy, $h\nu$ as shown in Eq. 2,

$$\alpha = \frac{\alpha_o (h\nu - E_g)^n}{h\nu} \quad (2)$$

where α_o is a constant, E_g is the optical band gap and n is a constant which depends on the probability of transition (it takes values as 1/2, 3/2, 2 and 3 for direct allowed, direct forbidden, indirect allowed and indirect forbidden transition, respectively) [18,32]. The band gaps of the AZO thin films were estimated by extrapolating to the photon energy axis, the linear portion of the Tuac's plot as shown in Figure 6.

The estimated optical band gap values show a marginal increase from 3.07 – 3.12 eV (undoped ZnO as reference) which was very sensitive to Al doping level as indicated by the inset of Fig. 6. When Al impurities were incorporated into ZnO (ie, Al:Zn = 1 at.%), there was a sudden lowering of band gap to 2.86 eV. Further increase in Al impurities to 2 at.% caused a widening of the band gap to 3.12 eV which later shrinked back to 3.07 eV at 5 at.% Al concentration as illustrated in Figure 6 (d). Such widening of optical energy band gap with Al doping have been described by Burstein–Moss effect [29,30,33]. Burstein-moss pointed out that an increase in the Fermi level in the conduction band of degenerate semiconductors leads to widening of the energy band (blue shift) [29,30]. Enhancement of band gap also ensures the successful doping of Al in the ZnO thin films [29,30,31].

On the other hand, the sudden lowering of band gap of AZO for Al:Zn = 1 at.% as earlier observed has been reported by Mohanty et al [26] and was explained in terms of stress relaxation mechanism. The reduction in slope of the linear portion of the Tauc plot observed for Al:Zn = 1 at.% suggests the introduction of defect states within the band gap. Thus, we interpret this shift due to merging of impurity band into the conduction band, thereby shrinking the band gap [26]. Formation of such impurity band giving rise to new donor electronic states just below the conduction band is possible and this arises due to hybridization between states of the ZnO matrix and of the Al dopant [26]. It seems that such formation of donor levels compensates the Burstein-Moss effect and results in the narrowing of the effective band gap of AZO. A reduction of stress on the film giving rise to widening of the band gap for 2 at.% Al concentration may also be due to enhanced thickness [30,31] of AZO film which may have some contribution to the observed blue-shift in the band gap [10]. Therefore the optical band gap of the AZO makes a peak increase at Al:Zn = 2 at.% which may obviously be the optimum doping concentration for AZO.

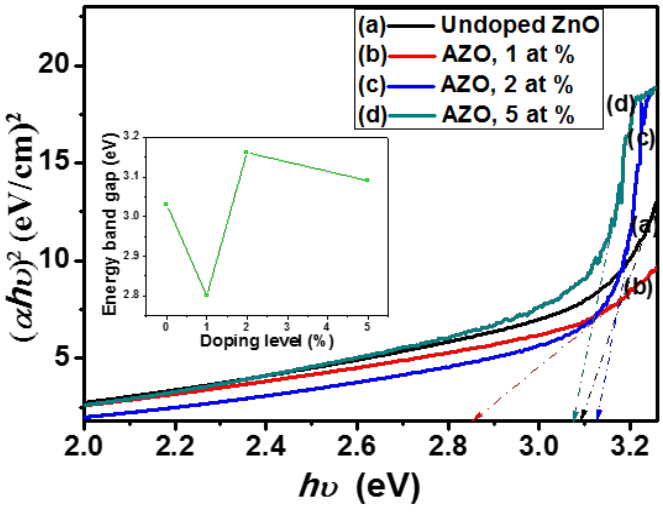

Figure 6. Tauc plot from absorbance spectra of AZO thin film for different Al concentrations. (a) 0 at.%. (b) 1 at.%. (c) 2 at.%. (d) 5 at.%. Inset shows the band gap trend with Al dopant variation in ZnO

4. Photo-electrochemical (PEC) Studies

Photoelectrochemical (PEC) response of a solar cell is based on the junction between semiconductor and an electrolyte [15,32]. The electrolyte plays an important role in PEC cell in acting as a medium for charge transfer between the photoelectrode and counter electrode [32,34]. The photoresponses of the AZO electrodes were studied by forming typical configuration cells, n-AZO (stainless steel substrate)/0.1 M Na_2SO_4/platinum/SCE as illustrated in Figure 7. These PEC solar cells are easy to fabricate because many processing steps of p–n junction have been simplified or eliminated. Since the junction with liquid is formed spontaneously upon contact, irregular shaped single crystal or thin films can be used [35]. The solution-based measurements allowed us to quickly test the quality of AZO film electrodes as solar cell materials [32].

4.1. Current-Voltage (I-V) Curves

The PV properties of AZO electrodes were studied by current-voltage measurement from the fabricated PEC solar cells. The current–voltage (I–V) characteristics of the annealed AZO thin films recorded in the dark and under illumination with 80 mW/cm^2 simulated white light are shown in Figure 8(a-c). A careful study of these photoresponse curves revealed that the dark current obtained at each AZO electrode was not zero however, very low values were seen. This observation may be ascribed to the fact that the cells might have been partially illuminated by the background light in the experimental room. When the electrodes were illuminated with white light, all photoelectrodes showed reasonably high photocurrent (short circuit current density, J_{SC}) densities with peak photocurrent density recorded for the electrode with Al:Zn = 2 at.%, as well as high open circuit voltages (V_{OC}). The anodic photocurrent varied remarkably with the concentration of Al in ZnO thus agreeing with previous characterizations of the AZO. Figure 8 also represents the chopped light tests carried out in order to study the photosensitivity of the thin films. The photosensitivity confirmed that AZO absorber is an n-type material and is useful for the solar cells [34]. It became clear in Figure 8 that the photoresponse of the electrodes increases with increase in concentration of Al and made a peak at 2 at.% as earlier observed. The measured values of the J_{SC} and V_{OC} with respect to Al doping are shown in Table 3.

It is however observed that the photocurrent densities and open circuit voltages for 1 and 5 at.% Al concentrations are relatively lower than that for 2 at.%. This may be due to some reasons earlier explained for XRD, surface morphology and optical characterizations, such as more compressive strain in the films at lower and higher doping levels which probably leads to a less dense nanostructures as illustrated in Figure 4 (b and d), and consequently low photoactivity [35]. The PEC measurement confirmed good photoactivities of the annealed AZO films prepared from simple CBD method. The photocurrent obtained in the present study is practically low for most applications requiring high values of current; however, it is well known that conversion efficiency of such film can be considerably scaled up by thermal, chemical and PEC surface treatments [35].

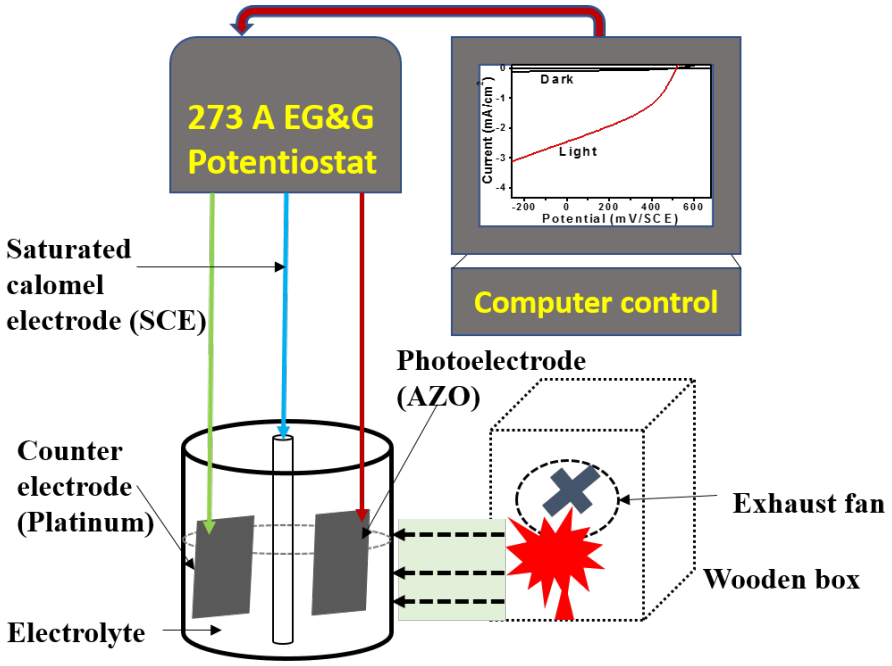

Figure 7. A schematic diagram showing photoelectrochemical current measurement set-up

Table 3. Measured and estimated parameters of the PEC solar cells of AZO thin film electrodes from *I-V* characteristic

AZO Electrodes with % Al	Photocurrent Density (J_{sc}) [μA/cm^2]	Photovoltage (V_{oc}) [mV]	J_{max} (μA/cm^2)	V_{max} (mV)	Efficiency, η (%)	Fill Factor (*FF*)
0	35.3	346	23.0	317	0.009	0.60
1	51.6	358	39.0	319	0.017	0.67
2	121.0	655	97.0	607	0.070	0.74
5	63.0	396	48.0	360	0.022	0.69

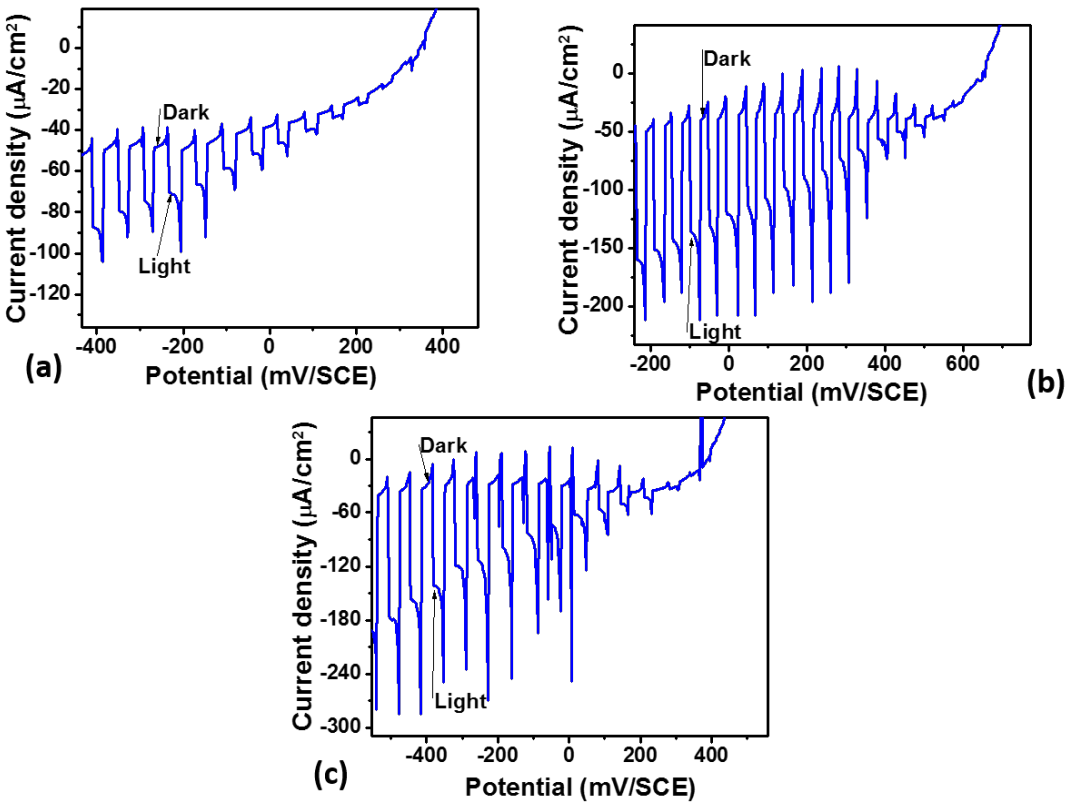

Figure 8. Current-Potential (*I-V*) curves of AZO thin films showing current and potential in the dark and under illumination for different Al concentrations (a) 1 at.% (b) 2 at.% and (c) 5 at.%

4.2. Power Conversion Efficiency (η) and Fill Factor (FF)

Energy or power conversion efficiency (η) of a solar cell is the percentage of power converted from absorbed light to electrical energy and collected, when a solar cell is connected to an electrical circuit [14]. The power outputs of the AZO electrode PEC solar cells in the current work were determined in the dark and under illumination with an input power (P_{in}), of 80 mW/cm^2. All the currents and potentials (J_{sc}, V_{oc}, J_{max} and V_{max}) measured for the AZO thin film electrodes are shown in the I-V curve of Figure 8 and the measured values are presented in Table 3, respectively. The light energy to electrical power conversion efficiency (η) and fill factor (FF) were estimated from the following Eqs.[21]:

$$\eta(\%) = \frac{J_{Max}(\mathrm{A/cm^2})V_{Max}(\mathrm{V})}{P_{in}(\mathrm{W/cm^2})} \times 100 \qquad (3)$$

$$\mathrm{FF} = \frac{J_{Max}(\mathrm{A/cm^2})V_{Max}(\mathrm{V})}{J_{SC}(\mathrm{A/cm^2})V_{OC}(\mathrm{V})}. \qquad (4)$$

The estimated values of power conversion efficiencies and fill factors for all the AZO film electrodes are presented in Table 3.

5. Conclusions

We have understudied the PV properties of AZO thin film electrodes synthesized by a novel chemical bath deposition technique under varied concentration of Al dopant in ZnO between 1 and 5 at.%. The synthesized thin films were characterized for thickness, structural, morphological and optical properties. The thickness profile of the thin films was found in the range of 5.50-10.15 μm which is suitable for PEC solar cell application. The XRD results revealed slight changes in the lattice parameters which occurred due to the successful substitution of Zn^{2+} by Al^{3+}. The result further indicates a clear enhancement in crystallinity at 2 at.% Al concentration which was adduced to stress reduction and other crystallographic defects in the film. SEM studies revealed densely grown nano-dendrites for 1 and 2 at.% Al concentrations with the densest nanostructure for Al:Zn = 2 at.%, having mean rod diameter of ~ 29 nm, and randomly oriented nanorods of mean diameter ~ 17 nm for 5 at.% Al concentration. The density and diameter of the nanostructures showed strong dependence on the concentration of Al dopant. UV-Vis spectrophotometry revealed a shift in absorption edge of approximately 50 nm into the visible band for the AZO nanostructures with 2 and 5 at.% Al concentrations which is a significant enhancement in optical properties of the films. Optical band gap energies varied between 3.07 – 3.12 eV upon Al doping. The synthesized AZO thin film electrodes showed tremendous n-type photoactivity in sodium sulphate (Na_2SO_4) electrolyte which motivate to check its feasibility in solar cell applications. The PV performance, studied by photocurrent-voltage characteristic revealed enhanced short circuit currents and open circuit voltages in the ranges of 35.3-121 μA/cm^2 and 346-655 mV, respectively. This yielded light energy to electrical energy conversion efficiencies and fill factors in the ranges of 0.009 - 0.070 % and 0.60 - 0.74. It is clear from this study

that AZO semiconductor materials are better materials for PEC solar cell applications than undoped ZnO.

Acknowledgements

M. D. Tyona sincerely thank the Thin Film Laboratory, Department of Physics, Shivaji University, Kolhapur for providing Laboratory facilities to support this research.

References

[1] Kim, K. H., Utashiro, K., Abe, Y., Kawamura, M., "Structural properties of zinc oxide nanorods grown on Al-doped zinc oxide seed layer and their applications in dye-sensitized solar cells", *Mater.,* 7, 2522-2533, 2014.

[2] El Manouni, A., Manjón, F.J., Mollar, M., Marí, B., Gómez, R., López, M.C., Ramos-Barrado J.R., "Effect of aluminium doping on zinc oxide thin films grown by spray pyrolysis", *Superlattices Microstruct.,* 39, 185-192, 2006.

[3] Hsu, C. H. and Chen, D. H., "CdS nanoparticles sensitization of Al-doped ZnO nanorod array thin film with hydrogen treatment as an ITO/FTO-free photoanode for solar water splitting", *Nanoscale Res. Lett.,* 7, 593-598, 2012.

[4] Becerril, M., Silva-López, H., Guillén-Cervantes, A., Zelaya-Ángel, O., "Aluminum-doped ZnO polycrystalline films prepared by co-sputtering of a ZnO-Al target", *Revista Mexicana De Física*, 60, 27-31, 2014.

[5] Alkahlout, A., Al Dahoudi, N., Grobelsek, I., Jilavi, M., de Oliveira, P. W., "Synthesis and characterization of aluminum doped zinc oxide nanostructures via hydrothermal route" *J. Mater.,* 235638, 1-8, 2014.

[6] Onkar Singh, Manmeet Pal Singh, Ravi Chand Singh., "Aluminum doping impact on morphology and sensing response of zinc oxide nanostructures", *The 14th International Meeting on Chemical Sensors,* 2012.

[7] Cebulla, R., Wendt, R., Ellmer, K., "Al-Doped Zinc Oxide films deposited by simultaneous RF and DC excitation of a magnetron plasma: Relationships between plasma parameters and structural and electrical film properties", *J. Appl. Phys*. 83, 1087-1095, 1998.

[8] Vanaja, A., Ramaraju, G. V. and Srinivasa Rao, K., "Structural and Optical Investigation of Al Doped ZnO Nanoparticles Synthesized by Sol-gel Process", *Ind. J. Sci. Technol.,* 9(12), 23-28, 2016.

[9] Kumar, B., Kim, S. W., "Energy harvesting based on semiconducting piezoelectric ZnO nanostructures", *Nano Energy*, 1, 342-355, 2012.

[10] Musat, V., Teixeira, B., Fortunato, E., Monteiro, R. C. C., Vilarinho, P., "Al-doped ZnO thin films by sol–gel method" *Surf. Coat. Technol.,* 180-181, 659-662, 2004.

[11] Lopes, T., Andrade, L., Ribeiro, H. A., Mendes, A., "Characterization of photoelectrochemical cells for water splitting by electrochemical impedance spectroscopy", *Int. J. Hydrogen Energy,* 35, 11601-11608, 2010.

[12] Hao, Y., Yang, M., Li, W., Qiao, X., Zhang, L., Cai, S., "A photoelectrochemical solar cell based on ZnO/dye/polypyrrole film electrode as photoanode' *Sol. Energy Mater. Sol. Cells*, 60, 349-359, 2000.

[13] Dharmadasa, I. M., Ojo, A. A., Salim, H. I., Dharmadasa, R., "Next Generation solar cells based on graded bandgap device structures utilising rod-type nano-materials", *Energies* 8, 5440-5458, 2015.

[14] Tyona, M. D., Osuji, R. U., Ezema, F. I., Jambure, S. B., Lokhande, C. D., "Enhanced photoelectrochemical solar cells based on natural dye-sensitized Al-doped zinc oxide electrodes", *Adv. Appl. Sci. Res.,* 7, 18-31, 2016.

[15] Grätzel, M., "Photoelectrochemical cells", *Nature,* 414, 338-344, 2001.

[16] Tyona, M. D., Osuji, R. U., Ezema, F. I., Jambure, S. B., Lokhande, C. D., "Highly efficient natural dye-sensitized photoelectrochemical solar cells based on Cu-doped zinc oxide thin film electrodes", *Adv. Appl. Sci. Res.,* 6, 7-20, 2015.

[17] Yousefi, M., Amiri, M., Azimirad, R., Moshfegh, A. Z., "Enhanced photoelectrochemical activity of Ce doped ZnO nanocomposite thin films under visible light", *J. Electroanal. Chem.,* 661, 106-112, 2011.

[18] Lee, S. H., Han, S. H., Jung, H. S., Shin, H., Lee, J., Noh, J. H., Lee, S., Cho, I. S., Lee, J. K., Kim, J., Shin, H., "Al-Doped ZnO thin film: A new transparent conducting layer for ZnO nanowire-based dye-sensitized solar cells", *J. Phys. Chem .C,* 114, 7185-7189, 2010.

[19] Yao, P. C., Hang, S. T., Lin, Y. S., Yen, W. T., Lin, Y. C., "Optical and electrical characteristics of Al-doped ZnO thin films prepared by aqueous phase deposition" *Appl. Surf. Sci.,* 257, 1441-1448, 2010.

[20] Al-Ghamdi, A. A., Al-Hartomy, O. A., El Okr, M., Nawar. A. M., El-Gazzar, S., El-Tantawy, F., Yakuphanoglu, F., "Semiconducting properties of Al doped ZnO thin films", Spectrochimica Acta, Part A, 131, 512-517, 2014.

[21] Zhao, X., Shen, H., Zhang, Y., Li, X., Zhao, X., Tai, M., Li, J., Li Jianbao, Li Xin, and Lin Hong, , "Aluminum-Doped Zinc Oxide as Highly Stable Electron Collection Layer for Perovskite Solar Cells", *Appl. Mater. Interfaces,* 8(12), 7826-7833, 2016.

[22] Wen-Wu Zhong, Fa-Min Liu, Lu-Gang Cai, Xue-Quan Liu, Yi Li, , "Effect of Growth Time on the Structure, Raman Shift and Photoluminescence of Al and Sb Codoped ZnO Nanorod Ordered Array Thin Films", *Appl. Surf. Sci*., 257, 9318- 9322, 2011.

[23] Yu, J., Yuan, Z., Han, S. and Ma, Z., "Size-Selected Growth of Transparent Well-Aligned ZnO Nanowire Arrays", *Nanoscale Res. Lett.,* 7, 517-525, 2012

[24] Wang, H. and Xie, C., "Controlled Fabrication of Nanostructured ZnO Particles and Porous Thin Films Via a Modified Chemical Bath Deposition Method", *J. Cryst. Growth,* 291, 187-196, 2006.

[25] Xia, Q.X., Hui, K.S., Hui, K.N., Hwang, D.H., Jai Singh, Cho, Y.R., Lee, S.K., Zhou, W., Wan, Z.P., Chi-Nhan Ha Thuc, Son, Y.G., "High quality p-type N-doped AZO nanorod arrays by an ammonia-assisted hydrothermal method", *Mater. Lett.,* 78, 180-183, 2012.

[26] Mohanty, B. C., Jo, Y. H., Yeon, D. H., Choi, I. J., and Cho, Y. S., "Stress-induced anomalous shift of optical band gap in ZnO:Al thin films", *Appl. Phys. Lett.* 95, 62103-62111, 2009.

[27] Shannon, R. D., "Revised effective ionic radii and systematic studies of interatomic distances in halides and chalcogenides", *Acta Crystallogr., Sect. A: Found. Adv.* 32, 751-767, 1976.

[28] Chow, L., Lupan, O., Chai, G., Khallaf, H., Ono, L., Roldan, K., Cuenya, B., Tiginyanu, I. M., Ursak, V. V., Sontea, V., Schulte, A., "Synthesis and characterization of Cu-doped ZnO one-dimensional structures for miniaturized sensor applications with faster response", *Sens. Actuators*, *A*, 189, 399-408, 2013.

[29] Burstein, E., "Anomalous optical absorption limit in InSb", *Phys. Rev.* 93, 632-647, 1954.

[30] Moss, T. S., "State-of-the-Art Program on Compound Semiconductors", *Proc Phys Soc London,* B67, 775-782, 1954.

[31] Tyona, M. D., Osuji, R. U., Asogwa, P. U., Jambure, S. B., Ezema, F. I., "Structural modification and band gap tailoring of zinc oxide thin films using copper impurities" *J. Solid State Electrochem.* 21, 2629-2637, 2017.

[32] Jayaprakashan, R., Hodes, G., "Non-aqueous electrodeposition of ZnO and CdO films", *Thin Solid Films,* 440, 19-27, 2003.

[33] Shinde, N. M., Deshmukh, P. R., Patil, S. V., Lokhande, C. D., "Aqueous chemical growth of Cu_2ZnSnS_4 (CZTS) thin films: Air annealing and photoelectrochemical properties", *Mater. Res. Bull.,* 48, 1760-1766, 2013.

[34] Lokhande, C. D., Pawar, S. H., "Electrochemical photovoltaic cells for solar energy conversion" *Mater. Chem. Phys.,* 11, 201-277, 1984.

[35] Scregg, J., Dale, P., Peter, L., Zopp, G., Forbes, L., "New routes to sustainable photovoltaics: evaluation of Cu_2ZnSnS_4 as an alternative absorber material", *Phys. Status Solidi A,* 245, 1772-1776, 2008.